Lifetimes of quasiparticle excitations in $4d$ transition metals: Scattering theory and LMTO-RPA-GW approaches

V. P. Zhukov,[1] F. Aryasetiawan,[2] E. V. Chulkov,[3] and P. M. Echenique[3]

[1]*Donostia International Physics Center (DIPC), Paseo Manuel de Lardizabal,4, 20018 San Sebastián, Spain*
[2]*Research Institute for Computational Sciences (RICS), National Institute of Advanced Industrial Science and Technology, AIST Tsukuba Central 2, 1-1-1 Umezono, Tsukuba, Ibaraki 305-8568, Japan*
[3]*Departamento de Fisica de Materiales and Centro Mixto CSIC-UPV/EHU, Facultad de Ciencias Químicas, Universidad del Pais Vasco/ Euskal Herriko Unibertsitatea, Apdo. 1072, 20018 San Sebastián/Donostia, Basque Country, Spain*

We report the theoretical studies of electron and hole lifetimes in Nb, Mo, Rh, Pd, Ag by means of an *ab initio* many-body GW method and of a semiempirical scattering-theory approach (STA). The GW approach includes the evaluation of band structures within the local-density approximation linear muffin-tin orbital TB formalism and employment of random-phase approximation in the calculations of the dielectric functions and screened Coulomb interaction. We show that the density-of-states (DOS) convolution model of the STA provides a good approximation to the *ab initio* averaged lifetimes, the energy dependence of the matrix element being rather unimportant. We discuss the role of the characteristics of electronic structure responsible for the deexcitation of hot electrons as well as the deviations of the *ab initio* lifetimes from the predictions of the free-electron gas model and the DOS convolution model .

PACS number(s): 73.20.At, 79.60.Bm, 79.60.Dp, 79.60.Ht

I. INTRODUCTION

The dynamics of low-energy electron excitations in metals is a key ingredient for the microscopic understanding of many chemical and physical phenomena on metal surfaces.[1] A number of experimental tools to study the dynamics of excited electrons have been elaborated. One of the most powerful techniques is the time-resolved two-photon photoemission spectroscopy (TR-2PPE), which allows us to measure the hot-electron lifetimes on a femtosecond scale.[2] Using this kind of spectroscopy, the hot-electron lifetimes have been measured for nonmagnetic metals,[3–8] magnetic transition metals,[9,10] high-Tc superconductors.[11]

Theoretical evaluations of lifetimes and related quasiparticle characteristics have been based mainly on the scattering-theory approach (STA) and on the self-energy formalism of many-body theory.[12–15] In the simplest version of the STA, the rate of hot-electron deexcitation is evaluated by using the convolution of the electron density of states (DOS). This convolution was used by Berglund and Spicer[16] in order to explain the experimental photoemission results in Cu and Ag. The scattering rates (inverse lifetimes) were first evaluated for silicon using the STA by Kane.[17] Later Krolikowski and Spicer[18] successfully employed STA to evaluate the density of states, the imaginary part of dielectric constant and the electron-electron scattering length from the experimental photoemission results in copper. Based on STA, Penn *et al* have analyzed the spin-polarized electron-energy-loss spectra and hot-electron lifetimes in ferromagnetic Fe, Ni, Co, and Fe-B-Si alloys.[19–22] In the paper by Passek *et al.*,[23] the experimental spin-dependent lifetimes of the $n=1$ image-potential state on Fe(110) have been reported and interpreted by invoking the convolution of the first-principle DOS. Based on the DOS convolution, Drouhin[24,25] has developed a model to evaluate the scattering cross section and spin-

dependent inelastic mean-free path and applied it to Cr, Fe, Co, Ni, Cu, Ag, Gd, Ta, Au. An analogous approach has been developed by Zarate *et al.*,[26] where simple approximations to the density of states have been used to obtain analytical expressions for the electron lifetimes in transition metals. In Ref. 10, an approach proposed before by Penn *et al.*[20] has been extended to include the generation of secondary electrons; the parameters of the model for the lifetime calculations have been evaluated for Fe, Co, Ni, Cu.

Although it is anticipated in the basic equations of the STA that within this approach nonempirical calculations are conceivable, practically they were never carried out because of a very large computational effort for transition matrix elements. So in all the cited references, the transition matrix elements were evaluated by fitting the calculated results to experimental data. The methods based on the self-energy formalism take explicitly into account the matrix elements and are more appropriate for the nonempirical applications. Such methods were first developed for the interacting free-electron gas model (FEG) by Quinn and Ferrell[27,29] who derived basic expressions for the hot-electron lifetimes within the random-phase approximation (RPA) for the polarization function. Analytical expressions for the lifetime in the limit of small energy–small density parameter were derived by Quinn and Ferrell,[27,29] and in the limit of small excitation energy by Ritchie and Ashley.[28] Some improvements in the lifetime calculations based on the FEG model have incorporated exchange and correlation effects,[30] realistic electron densities within a statistical approximation[31] and band-structure effects.[32]

In the last years, first-principle calculations of quasiparticle lifetimes have been performed.[33–38] In such methods, the electron self-energy is usually evaluated by employing the so-called GW approximation[12–15] of the many-body theory. The first step of such approach includes the evaluation of the band structure of a solid, usually within the local-density

approximation (LDA). Then within the RPA the density response functions is calculated and used to evaluate the dielectric functions and screened Coulomb interactions. Finally, either matrix elements of the self-energy operator are calculated on the energy shell or Dyson equation is solved to get the self-energy corrections to the LDA eigenvalues.

Such calculations have been performed for electron quasiparticles in magnesium and beryllium,[37] aluminum,[33,37] copper, silver, and gold[33,37] and for hole quasiparticles in copper and gold.[36] All these researches used the LDA pseudopotential approach and the plane-wave Bloch basis set (PPW-RPA-GW). Recently the lifetimes of electrons and holes in copper, silver, and gold have been also calculated within the LMTO (linear muffin-tin orbital)-RPA-GW approach,[38] i.e., using a set of numerical muffin-tin orbitals to construct the basis Bloch functions. In spite of the differences in the calculation formalisms, a good accordance between the results of different calculations was obtained for electron quasiparticles.

The RPA-GW calculations, in general, correctly reproduce the trends observed in the experimental lifetimes, although noticeable discrepancies between the experimental and theoretical data still remain at some excitation energies.[35,38] The performed *ab initio* theoretical evaluations refer, however, to a narrow class of metals with specific electronic band structure that includes free-electron-like states at the Fermi level E_F (Al, Be, Mg, Cu, Ag, Au), and localized d states well below E_F (Cu, Ag, Au). For metals with non-localized d states at E_F, no attempts have been made to evaluate the decay rates. The experimental data exist only for the quasiparticle lifetimes in Rh and Ta.[39]

The comparison of the quasiparticle lifetimes in noble metals calculated by means of the LMTO-RPA-GW method with experimental data and with the results of the PPW-RPA-GW calculations[38] have shown a good reliability of the LMTO evaluations. Besides, the LMTO-RPA-GW method does not require very long plane-wave basis sets that are necessary to approximate well the dielectric functions of the metals. So we believe that LMTO-RPA-GW approach possesses predictive virtues, and report in this paper the quasiparticle lifetime calculations for the $4d$ transition metals Nb, Mo, Rh and Pd. One of the goals of our study is to reveal if there are important differences in the quasiparticle lifetimes between these metals and the noble metals, extensively studied before, and to understand, as far as possible, the origins of such differences. So we use here comparisons with the previously evaluated data on the quasiparticle damping in Ag.[38,40]

Although the *ab initio* methods have, in principle, high predictive possibilities, their applications are limited by the big amount of computations required. At the same time, the semiempirical versions of STA have also proven to be very useful to understand various dynamic properties of excited electrons. So we also discuss the possibility of accurate description of the lifetimes in Nb, Mo, Rh, Pd by using the DOS convolution model of STA.

In Sec. II of the paper, we discuss the methods of the lifetime calculations within the STA and GW approaches. In Sec. III, we analyze the precision of the calculations for dielectric functions of the metals of interest by comparing them with the available optical data. In Sec. IV, we present the results of the *ab initio* LMTO-RPA-GW lifetime calculations and discuss the factors responsible for the distinctions between the damping of electrons in the metals of interest and in the noble metals. In the same section, we obtain the parameters of the STA model by fitting the data computed by STA to the results of our *ab initio* calculations. The origin of the discrepancies between the results of the two approaches is also discussed. The conclusions are addressed in Sec. V.

II. THE METHODS OF EVALUATING THE HOT-ELECTRONS LIFETIMES

For decades, the evaluations of the quasiparticle lifetimes have been performed using equations based on the interacting FEG model.[27–29] In the limit of a small electron-density parameter r_s (degenerate electron gas) and a small quasiparticle energy E with respect to the Fermi level E_F, the lifetime is reduced to the simple expression[29]

$$\tau = 263 r_s^{-5/2} (E - E_F)^{-2} (\text{fs eV}^2), \quad (1)$$

which assumes that the so-called scaled lifetime $\tau \times (E - E_F)^2$ is energy independent and determined only by the r_s density parameter. An energy scaling qualitatively similar to that of Eq. (1) has been observed for electrons in the free-electron-like band-states of noble metals.[34,35]

In general, more possibilities are provided by the scattering-theory approach, where no limitations are imposed on the shape of charge density. In the STA, the decay rate of an initial state $\phi_i(\mathbf{r})$ at the energy E_i is determined by the probability of the primary electron scattering into a final state $\phi_f(\mathbf{r})$ at the energy E_f. It is accompanied by a secondary electron excitation from an occupied initial state $\phi_{i'}(\mathbf{r})$ at the energy E_i' into an unoccupied state $\phi_{f'}(\mathbf{r})$ at the energy $E_{f'}$. In the first order of the time-dependent perturbation theory and by using the "golden rule" this probability is written as (we use afterwards atomic units: $m_e = e^2 = \hbar = 1$) [41]

$$P_{i,i'}^{f,f'} = 2\pi |[W(E_i - E_f)]_{i,i'}^{f,f'}|^2 \delta(E_i - E_f + E_{i'} - E_{f'}). \quad (2)$$

Here W is the matrix element of the dynamic screened interaction

$$[W(\omega)]_{i,i'}^{f,f'} = \int d\mathbf{r} \, d\mathbf{r}' \, \phi_i^*(\mathbf{r}) \phi_{i'}^*(\mathbf{r}')$$
$$\times W(\mathbf{r} - \mathbf{r}', \omega) \phi_f(\mathbf{r}) \phi_{f'}(\mathbf{r}'). \quad (3)$$

Due to excessive complications that arise with the integration in Eq. (3), further simplifications are usually made. It is supposed that the matrix element in Eq. (3) can be replaced by its averaged value, traditionally denoted as $M(\omega)$, which depends only on the energy loss of the primary electron $\omega = E_i - E_f$ (so-called random-k approximation[17]). After neglecting the exchange terms contained in Eq. (3),[20] performing angular averaging in Eq. (3) and summation over all the possible scatterings of primary and secondary electrons

one arrives at the following basic expression for the scattering rate of a hot electron of the energy E and spin σ:

$$\frac{1}{\tau_\sigma(E)} = 2\pi \int_{E_F}^{E} dE' \rho_\sigma^>(E') \int_{E_F-\omega}^{E_F} d\varepsilon \times [\rho_\sigma^<(\varepsilon) \rho_\sigma^>(\varepsilon+\omega)$$

$$+ \rho_{\bar\sigma}^<(\varepsilon) \rho_{\bar\sigma}^>(\varepsilon+\omega)] |M(\omega)|^2. \quad (4)$$

Here $\omega = E - E'$ is the energy loss in the primary electron deexcitation, and $\rho^>(E) = [1-f(E)]\rho(E)$, $\rho^<(E) = f(E)\rho(E)$ where $f(E)$ is the Fermi-Dirac occupation function and $\rho(E)$ is the density of states. Hereafter, the model provided by Eq. (4) is referenced as the DOS convolution model. One can suppose that within a small energy interval, the matrix element M is fairly constant. Although such supposition has no general theoretical justifications, it has been successfully used in many researches based on the STA approach.[23–26] The most drastic simplification of the STA is achieved when one assumes that not only the matrix element but also the DOS takes a constant value ρ_S:[21]

$$\frac{1}{\tau_\sigma(E)} = \pi \rho_S^3 |M|^2 (E - E_F)^2. \quad (5)$$

The similarity between this equation and Eq. (1) allows us to express the matrix element $|M|^2$ in terms of the FEG theory.[29] This expression has served as a basis in many qualitative discussions because it provides a very simple model of damping in which only two factors play the role in the decaying of a quasiparticle: the transition matrix element and the phase space available for the primary electron transitions $[\rho_S^3 (E - E_F)^2]$.

In order to achieve a quantitative agreement with experimental data on the lifetimes in transition metals, it is necessary, however, to distinguish between s, p, and d states, so a number of improved models have been proposed. In the work by Zarate *et al.*,[26] it was supposed that the matrix elements are energy independent but different for the transitions of electrons between s, p, and d states, which has allowed to determine the transition-matrix elements by fitting to the experimental lifetimes. An analogous approach has been used in Refs. 24,25. Considering that the DOS convolution model of the STA employs physically simple values, the possibility of using this model for a description of the hot electron dynamics in solids with intermediately localized d states is very appealing. However, the degree of the d-electron localization and the features of DOS change noticeably from Nb to Pd, and they are very different from those observed in noble metals. So even the feasibility of a broad use of such a model is questionable. In this paper, we analyze this problem by performing comparisons with the LMTO-RPA-GW results. Such comparisons permit us to reveal the factors that govern the distinctions between the quasiparticle damping in Nb, Mo, Rh, Pd and in the noble metals and to clarify the limitations of the DOS convolution model. Besides, they permit us to understand, to a certain extent, the origin of the lifetime changes within the series of metals of interest.

We have performed *ab initio* calculations of the quasiparticle lifetimes by means of the LMTO-RPA-GW approach.[42–46,13,38,47] The polarization function of a solid is evaluated within the RPA approximation[13]

$$\mathbf{P}_{i,j}(\mathbf{q},\omega) = \sum_{\sigma,t,\mathbf{k}} \sum_n^{occ} \sum_{n'}^{unocc} \frac{1}{t\omega - \epsilon_{\mathbf{k}+\mathbf{q},n'} + \epsilon_{\mathbf{k},n} + i\delta}$$

$$\times \langle B_{\mathbf{q},i}\psi_{\mathbf{k},n}|\psi_{\mathbf{k}+\mathbf{q},n'}\rangle \langle \psi_{\mathbf{k}+\mathbf{q},n'}|\psi_{\mathbf{k},n}B_{\mathbf{q},j}\rangle, \quad (6)$$

with i,j being the indices of basis Bloch states, and n,n' being the band indices. The summation includes terms with $t = \pm 1$ (electrons and holes) and spin value σ. To calculate the single-particle states of a solid $\psi_{\mathbf{k},n}$, we employ the LMTO method in the basis of tight-binding muffin-tin orbitals.[43] The basis Bloch functions $B_{\mathbf{q},i}$ of the polarization matrix and of all the subsequent many-body calculations are composed from the products of the muffin-tin orbitals by using the procedures of orthogonalization described in Ref. 45. Once the polarization matrix is obtained, we evaluate the density-density response function matrix $\mathbf{R}$, dielectric and inverse dielectric matrices, ϵ and ϵ^{-1}, and calculate the matrix of the screened Coulomb interaction $\mathbf{W}$,

$$\mathbf{R} = \mathbf{P} + \mathbf{P} \cdot \mathbf{v} \cdot \mathbf{R}, \quad (7)$$

$$\epsilon = \mathbf{1} - \mathbf{v} \cdot \mathbf{P}, \quad (8)$$

$$\epsilon^{-1} = \mathbf{1} + \mathbf{v} \cdot \mathbf{R}, \quad (9)$$

$$\mathbf{W} = \epsilon^{-1}\mathbf{v}. \quad (10)$$

The Coulomb potential matrix $\mathbf{v}$ is computed by the method desribed in Ref. 45. We calculate the self-energy within the GW approximation of the many-body theory[14] retaining the first member in the series expansion of Σ in terms of the screened Coulomb interaction W:

$$\Sigma(\mathbf{r},\mathbf{r}',\omega) = \frac{i}{2\pi}\int d\omega' G(\mathbf{r},\mathbf{r}',\omega+\omega')W(\mathbf{r},\mathbf{r}',\omega'). \quad (11)$$

In this approach the self-energy is obtained by replacing the full Green function by the Green function of noninteracting electrons; the imaginary part of the correlation contribution in self-energy is expressed as[13]

$$\text{Im}\,\Delta\Sigma_{\mathbf{q},n}^c(\omega) = \sum_{\mathbf{k}} \sum_{n'}^{occ} \sum_{i,j} \text{Im}\,W_{i,j}^c(\mathbf{k}, \epsilon_{\mathbf{k}-\mathbf{q},n'} - \omega)$$

$$\times \langle \psi_{\mathbf{q},n}\psi_{\mathbf{k}-\mathbf{q},n'}|B_{\mathbf{k},i}\rangle$$

$$\times \langle B_{\mathbf{k},j}|\psi_{\mathbf{k}-\mathbf{q},n'}\psi_{\mathbf{q},n}\rangle\Theta(\epsilon_{\mathbf{k}-\mathbf{q},n'} - \omega), \quad (12)$$

when $\omega \leqslant \mu$, and

$$\text{Im}\,\Delta\Sigma_{\mathbf{q},n}^c(\omega) = -\sum_{\mathbf{k}} \sum_{n'}^{unocc} \sum_{i,j} \text{Im}\,W_{i,j}^c(\mathbf{k}, \omega - \epsilon_{\mathbf{k}-\mathbf{q},n'})$$

$$\times \langle \psi_{\mathbf{q},n}\psi_{\mathbf{k}-\mathbf{q},n'}|B_{\mathbf{k},i}\rangle \langle B_{\mathbf{k},j}|\psi_{\mathbf{k}-\mathbf{q},n'}\psi_{\mathbf{q},n}\rangle$$

$$\times \Theta(\omega - \epsilon_{\mathbf{k}-\mathbf{q},n'}), \quad (13)$$

when $\omega > \mu$.

Here $W^c = W - v$ is the correlation part of the screened potential. The expectation values of the operator $\Delta\Sigma(\omega) = \Sigma(\omega) - V_{LDA}^{xc}$, where V^{xc} is the LDA exchange-correlation potential, determine the many-body self-energy corrections to the LDA eigenvalues $\epsilon_{\mathbf{q},i}$ through the Dyson's equation

$$E_{\mathbf{q},i}(\omega) = \epsilon_{\mathbf{q},i} + \langle \psi_{\mathbf{q},i} | \Delta\Sigma_{\mathbf{q},i}(\omega) | \psi_{\mathbf{q},i} \rangle. \qquad (14)$$

The real part of the self-energy expectation value is calculated by the Hilbert transform. The solution of Dyson's equation is simplified when only the linear part of the dependence of Re $\Delta\Sigma$ on ω is retained and the change of Im $\Delta\Sigma$ with ω is neglected. In this approximation, the self-energy corrections are

$$\Delta\epsilon_{\mathbf{q},i} = E_{\mathbf{q},i} - \epsilon_{\mathbf{q},i} = Z_{\mathbf{q},i}\Delta\Sigma_{\mathbf{q},i}(\epsilon_{\mathbf{q},i}), \qquad (15)$$

where

$$Z_{\mathbf{q},i} = \left[1 - \frac{\partial \, \mathrm{Re}\, \Delta\Sigma_{\mathbf{q},i}(\omega)}{\partial \omega} \right]^{-1}_{\omega = \epsilon_{\mathbf{q},i}}, \qquad (16)$$

is the so-called renormalization factor. The imaginary part of the self-energy correction gives then the linewidth of the quasiparticle excitation, and the inverse value determines the lifetime of a quasiparticle[15]

$$\tau_{\mathbf{q},i}^{-1} = 2|\mathrm{Im}\,\Delta\epsilon_{\mathbf{q},i}|. \qquad (17)$$

For a given excitation energy we average the calculated lifetimes over $\mathbf{q},i$. Then substituting the *ab initio* densities of states and averaged lifetimes into Eq. (4), we evaluate the STA energy-dependent matrix elements and choose the energy-independent matrix elements optimal inside the energy interval between 1 and 5 eV.

The FEG theory lifetimes used in the discussions of Sec. IV were calculated by numerical integration of the equations of conventional theory with the Lindhard's RPA polarization function.[14,29]

III. DIELECTRIC FUNCTIONS AND ELECTRON-ENERGY-LOSS SPECTRA

Since the dielectric function determines the screened Coulomb interaction and consequently the quasiparticle self-energy, the precision in the calculations of dielectric function is very important for the correct *ab initio* GW lifetime evaluations. Previous studies have shown that some errors may
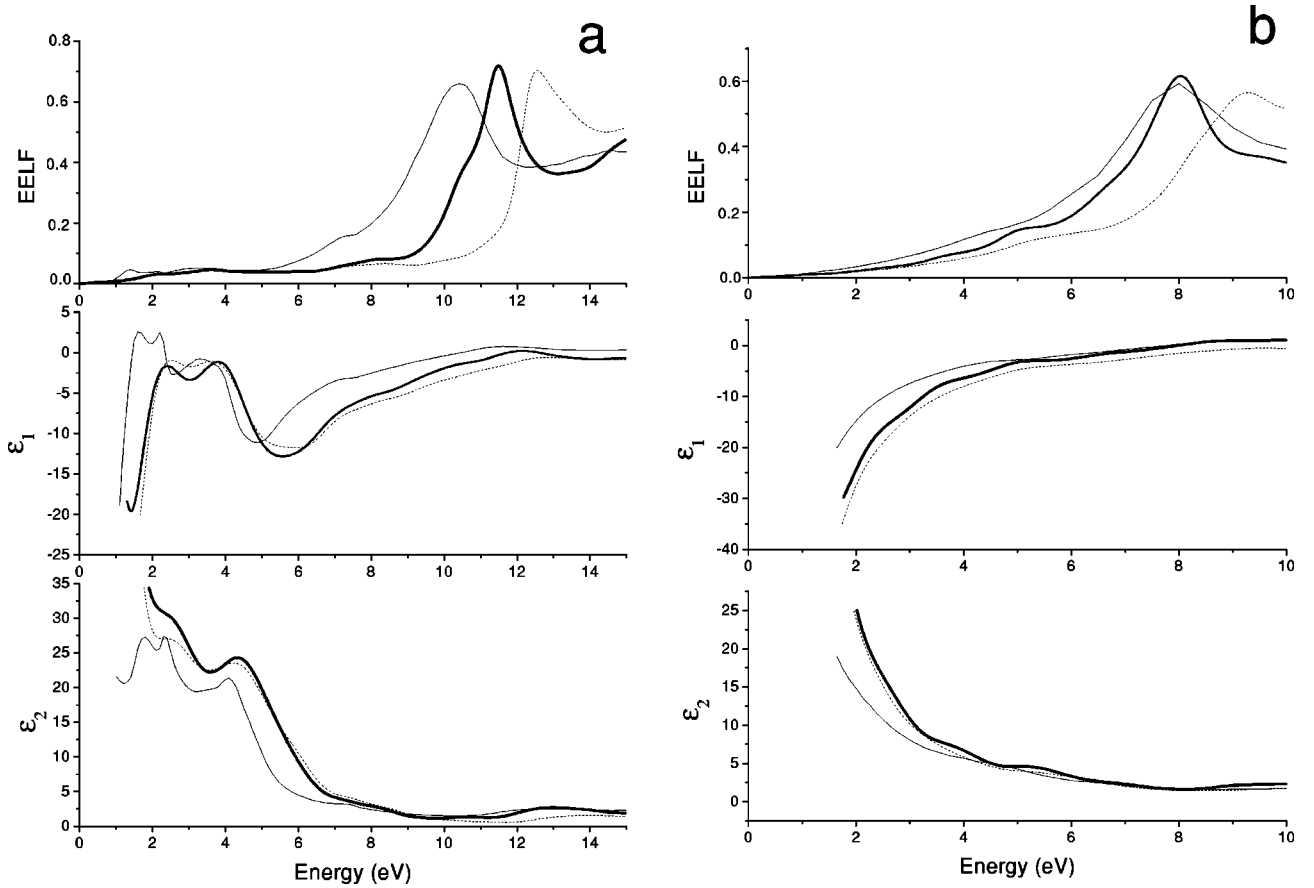

FIG. 1. The experimental (thin solid lines) and calculated (thick solid lines and dashed lines) electron-energy loss function (EELF) as well as real and imaginary parts of dielectric function of Mo (panel a) and Pd (panel b). Thick solid line represent the data with the $4f$ states included in the basis set, whereas dashed lines show the results with the $4f$ states omitted.
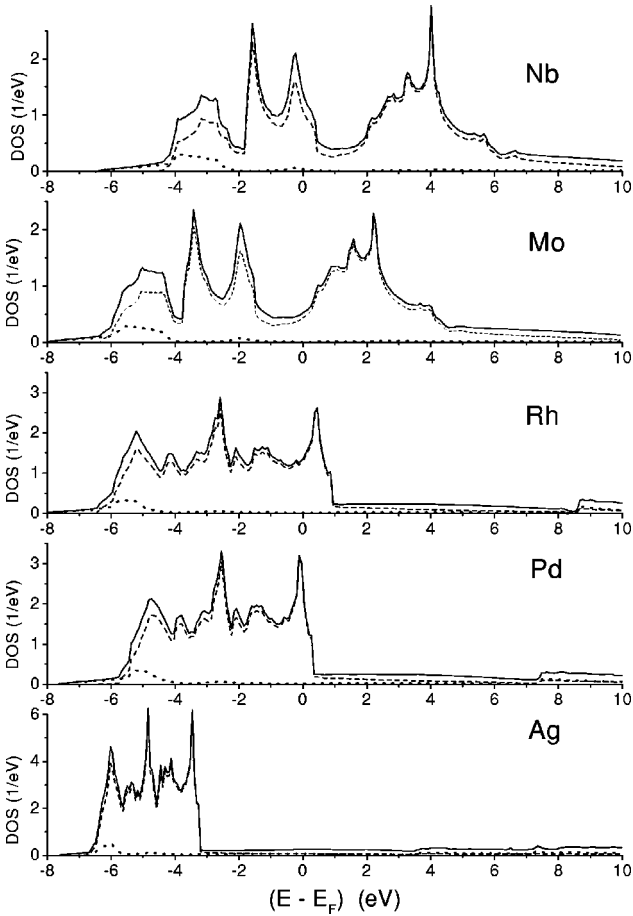
FIG. 2. The total and partial densities of states in Nb, Mo, Rh, Pd, Ag as calculated by the LMTO method. Total DOS's are shown by solid lines, the $4d$ DOS are shown by dashed lines, and the $5s$ DOS by dotted lines
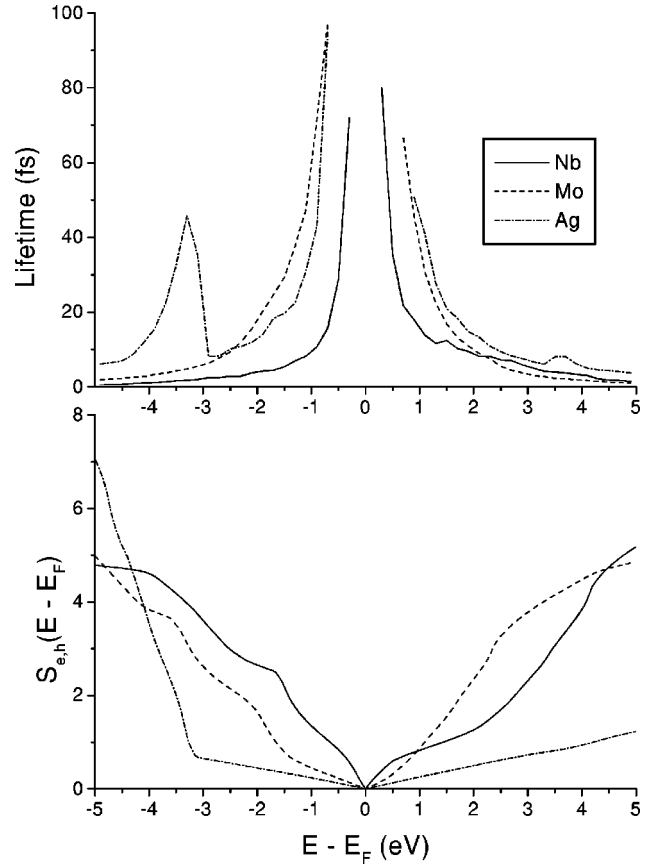

FIG. 3. Upper panel: the averaged quasiparticle lifetimes in Nb, Mo, Ag as calculated by the LMTO-RPA-GW approach. Lower panel: the number of states participating in the quasiparticle damping (see text).

occur in the dielectric functions because of the drawbacks of the LDA approach in the calculations of the crystal orbitals.[38,48,49] For example, the onset energy of the interband s-d transitions in the imaginary part of dielectric function of Ag calculated by the conventional LDA methods is about 1 eV higher than the corresponding experimental value. Besides, the peak of plasmon absorption in Ag is absent if the electron-energy loss function (EELF) is calculated by using the standard LDA band structure.[48] These drawbacks of the LDA approach have been corrected in the LMTO calculations of Ref. 38 by changing the continuous quantum number of d states; here we compare the lifetime data of Ref. 38 with our new data on Nb, Mo, Rh, Pd.

Another factor that can influence the precision of the dielectric functions and quasiparticle lifetime calculations is the choice of the basis states used in the calculations of the polarization matrix. As follows from the results of the lifetime calculations for Ni, Ref. 46, the $4f$ states, together with the $3d,4s,4p$ states have to be included into the product-orbital basis functions in order to get in a broad energy range a correct description of the dielectric functions of the $3d$ transition metals. However, for a reliable averaging of lifetimes over wave vectors, a very big number of the vectors

has to be used, so the employment of the minimal set of orbitals, i.e., $(n-1)d,ns,np$, is desirable. We performed the calculations within the minimal basis set and with the $4f$ functions included, and in Figs. 1(a) and 1(b) we show the dielectric functions and the EELF calculated for bcc Mo and for fcc Pd. They are compared with the experimental data derived from optical measurements.[50] The dielectric functions of Nb and Rh are very similar to those of Mo and Pd, respectively.

The calculated real and imaginary part of the Mo dielectric function, Fig. 1(a), are in qualitative agreement with the corresponding experimental data. The calculations reproduce the changes of the experimental data with energy, although the energies of local maxima in the calculated ϵ_1 and ϵ_2 differ from the energies of the experimental maxima by 0.6–1.0 eV.

The greatest differences between the calculated and experimental data on EELF of Mo are connected with the plasmon absorption: optical measurements show the absorption maximum at 10.4 eV, whereas the calculated plasmon absorption peak has the energy of the maximum 11.5 eV with inclusion of the basic $4f$ states and 12.5 eV without $4f$ states. However, these differences are observed at the energies well above the energy range of interest 0–5 eV. The discrepancies between experimental and calculated data do
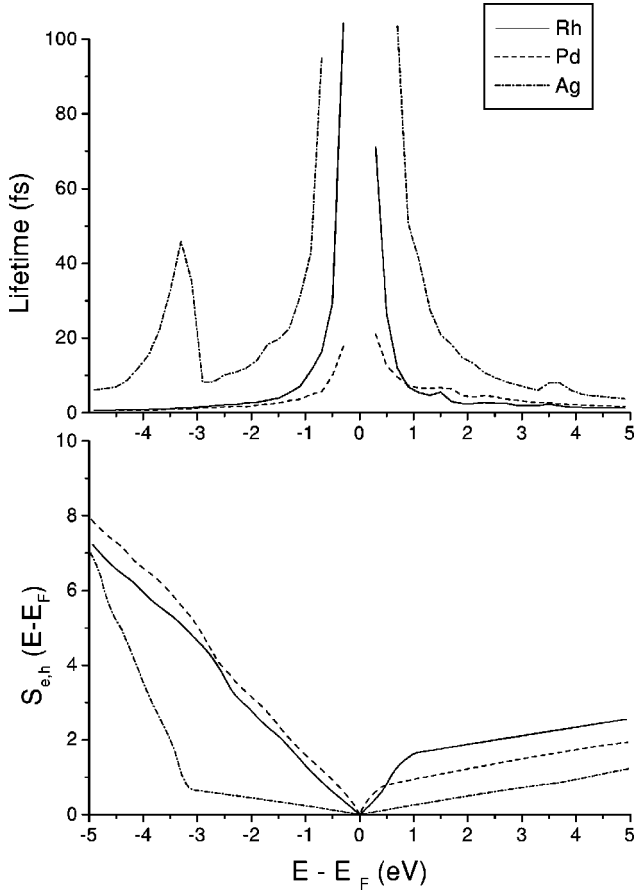
FIG. 4. Upper panel: the averaged quasiparticle lifetimes in Rh, Pd, Ag as calculated by the LMTO-RPA-GW approach. Lower panel: the number of states participating in the quasiparticle damping (see text).
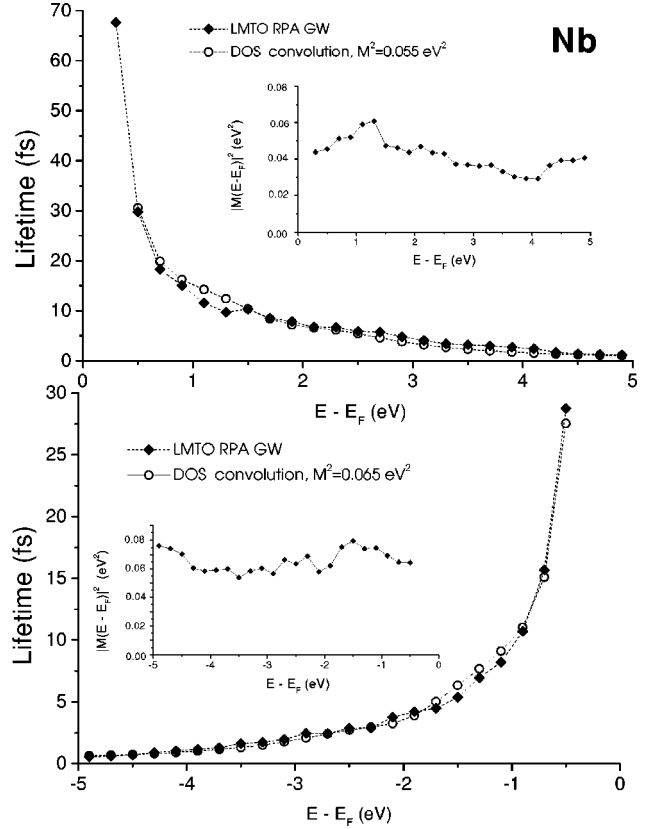

FIG. 5. The averaged electron (upper panel) and hole (lower panel) quasiparticle lifetimes in Nb. The results of the LMTO-RPA-GW calculations are shown by solid diamonds. The open circles represent the results of the DOS convolution model with fixed matrix element (see text). The insets show the energy dependence of the matrix element of the DOS convolution model evaluated by adjusting to the LMTO-RPA-GW lifetimes.

not generally exceed those of the previous calculations for noble metals[38] where a good correspondence between LMTO-RPA-GW, PPW-RPA-GW and lifetime experimental data has been achieved. For energies up to 5 eV, the EELS and dielectric functions calculated within the minimal basis set of $s \times s, s \times p, s \times d, p \times d$ products agree well with the data obtained by including also products with 4f orbitals. Thus, the possibility of using the minimal basis set for lifetime evaluations at low energy is well confirmed.

The EELF and dielectric function of Pd, Fig. 1(b), calculated with 4f orbitals included agree with experimental data better than those of Mo. For the energies up to 5 eV, our calculations for Pd show better agreement with experiment than the previous calculated data of Ref. 51, where the EELF was underestimated, and of Ref. 52, where it was overestimated.

IV. QUASIPARTICLE LIFETIMES

In Fig. 2, we show the densities of states of the bcc Nb, Mo and fcc Rh, Pd, and Ag, which helps us to understand the differences between the quasiparticle lifetimes in these metals and in the noble metals. The major peaks of the DOS correspond to the contributions of the 4d states that are shown in Fig. 2 by the dashed line. In Nb the bands of d states lie in the energy interval from -4 eV to 6 eV whereas in Mo they are shifted down by 2 eV. (Here and in the following, all the energies are given with respect to the Fermi level.) The tail of the DOS at the energy below the 4d states belongs to the valence 5s states whose contributions are shown by the dotted lines. The lower bands of the d states are hybridized with the s states. So the contribution of the s states is noticeable for energies up to -2 eV in Nb, -4 eV in Mo, Rh, Pd and up to -5.7 in Ag. The DOS at the energy above the energy of d bands corresponds to the hybridized bands composed by the 5p and 4d states. On going from Nb to Ag, one observes an increase in the localization of d states that leads to the narrowing of these bands and shifts them to lower energy. At the same time, the contribution of the d bands to the hybridized p,d bands decreases. So the d bands in Ag are the most localized ones, whereas the Ag 5p bands are the most free-electron-like.

The calculated lifetimes averaged over the wave vectors are shown in Figs. 3,4. In these figures we also plot the $S_{e,h}(E)$ values that are equal to the number of states lying in the energy interval between the Fermi level and the excita-
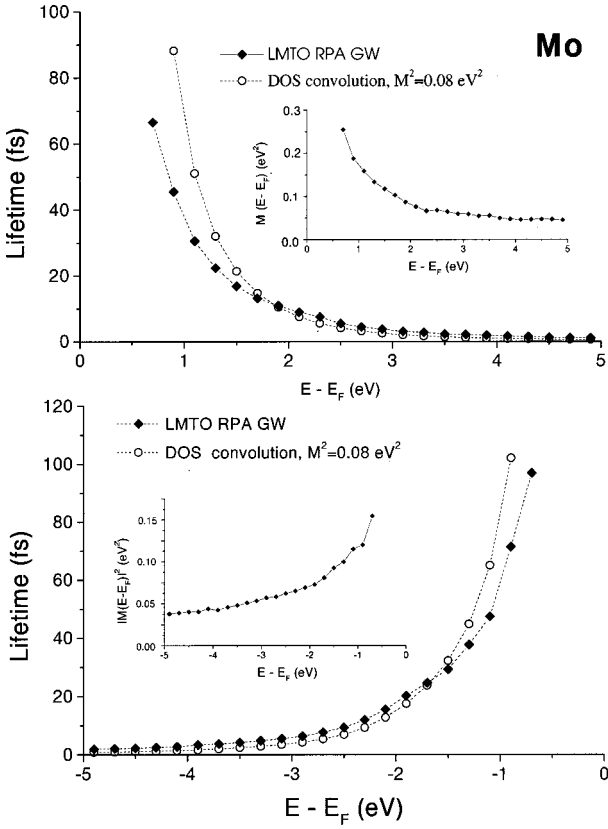
FIG. 6. The averaged lifetimes of electron (upper panel) and hole (lower panel) quasiparticles in Mo. Designations correspond to Fig. 5.
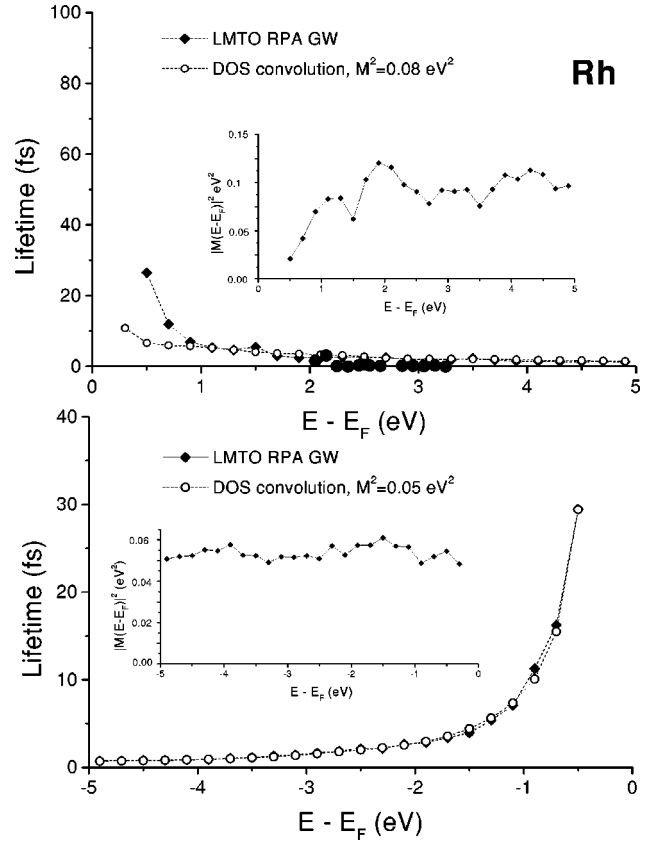

FIG. 7. The averaged lifetimes of electron (upper panel) and hole (lower panel) quasiparticles in Rh. Designations correspond to Fig. 5. The solid circles in the upper panel represent the experimental relaxation times.

tion energy E. So these values represent the phase space available for the quasiparticle damping. As it follows from the character of the DOS, the damping of both electron and hole quasiparticles in Nb and Mo is realized through the transitions of primary electrons (holes) from their initial $4d$ states into final $4d$ states. The initial and final states of electron quasiparticles in Ag are free-electron-like $5p$ states that have the DOS much lower than that of Nb and Mo. It follows then from the lower panel of Fig. 4 that due to this difference in the DOS the phase space of electron quasiparticles damping in Ag is noticeably lower than the phase space of the damping in Nb, Mo. So one can expect that the electron quasiparticle lifetime is longer in Ag than in Nb, Mo, which is well confirmed by Fig. 4. Similar phase-space arguments are also applicable to explain the lower values of the electron quasiparticle lifetimes in Rh and Pd compared to those in Ag. The available experimental data on Rh,[39] shown in Fig. 7, also well confirm the small lifetime values.

Attempts to invoke the phase-space arguments to explain the differences between the hole lifetimes in Ag and in the other metals encounter, however, some problems. Comparing the hole lifetimes in Rh, Pd, and Ag, Fig. 4, one can see that the bigger volume of the hole damping phase space in Rh and Pd is consistent with the smaller hole lifetimes. It follows from Fig. 3 that the phase space of the hole damping in Ag at the energies above -4 eV is lower than that in Nb, Mo. However, the lifetimes of the p holes in Ag at the energy

higher than -3 eV appears to be shorter than the lifetimes of holes in Mo. Besides, in Ag at the energy about -3 eV, a sudden change of the hole lifetimes appears. It is not related with the available phase space at all, and it is explained by the small values of transition-matrix elements between the initial d states and final s, p states.[38] An attempt to explain the differences between the lifetimes in Nb and Mo also turns out to be problematic. In this case, the smaller electron lifetime in Nb at the energy between 1 and 2 eV is in conflict with the smaller phase volume.

Hence, phase-space arguments appear to be of limited validity in explaining the differences between the quasiparticle lifetimes in the metals of interest. More successful is the DOS convolution model of the STA that we comment in the following. In Figs. 5–9, we show the results of adjusting the lifetimes calculated by using Eq. (4) to the averaged *ab initio* lifetimes. The LMTO-RPA-GW lifetimes averaged over all the wave vectors implicitly include complicated bandstructure effects. As it follows from the insets in Figs. 5–9, most parts of the changes in the calculated STA matrix elements cannot be directly related with the features of the band structures. Only in the case of electron quasiparticle in Ag a sudden change in $|M(\omega)|^2$ at the energy about 3.5 eV corresponds to a band-structure effect noticeable in the lifetime curve at the same energy. Besides, the jump of $|M(\omega)|^2$ at
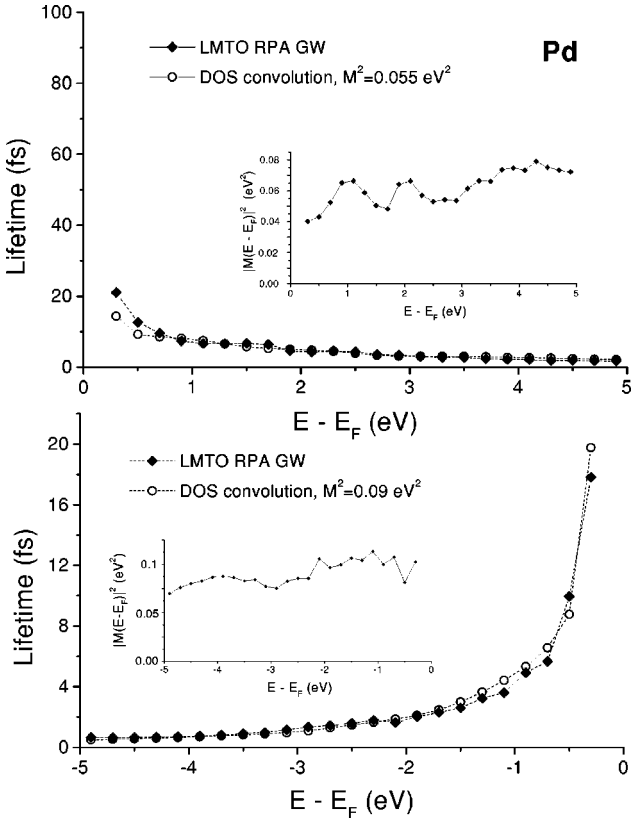
FIG. 8. The averaged lifetimes of electron (upper panel) and hole (lower panel) quasiparticles in Pd. Designations correspond to Fig. 5.

FIG. 9. The averaged lifetimes of electron (upper panel) and hole (lower panel) quasiparticles in Ag. Designations correspond to Fig. 5.

the energy about -3 eV is associated with the top d bands. Nevertheless, the variations in the matrix element, although being larger than in the previous evaluation for silicon,[17] appear to be rather unimportant in Nb, Mo, Rh, and Pd. Both the electron and hole lifetimes calculated by the LMTO-RPA-GW approach in most cases agree well with the lifetimes evaluated by Eq. (4) with constant matrix elements. For electron and hole excitations in the p states of Ag, i.e., at the energy above -3 eV, the agreement is also good, and only in the top d states at the energy below -3 eV the STA and the LMTO-RPA-GW results separate, due to the importance of the transition-matrix elements.[38]

Some fine relations between the calculated lifetimes of electrons and holes are illustrated by Figs. 10,11 where we show the ratios of electron and hole lifetimes in the metals of interest. The trends observed in the LMTO-RPA-GW values of $\tau_e(\mathrm{Nb})/\tau_e(\mathrm{Mo})$, and $\tau_h(\mathrm{Rh})/\tau_h(\mathrm{Pd})$ are well reproduced by the DOS convolution model, while for the value $\tau_h(\mathrm{Nb})/\tau_h(\mathrm{Mo})$ an essential divergence is observed above 3 eV. This divergence can be explained by the differences in the band states at the energy below -3 eV. As it follows from Fig. 2, at such energy the energy bands of Nb contain noticeable contribution of the Nb s states. So, when the energy of a band state becomes lower than this threshold, the matrix element of the transitions between the given state and the d states of higher energy should change, therefore, the approximation of the constant matrix element is less valid.
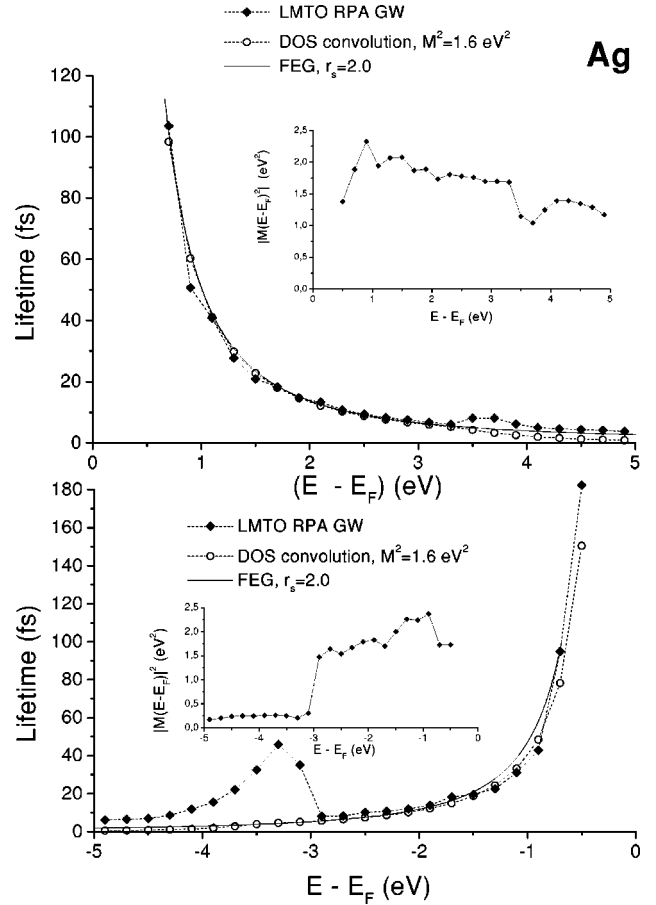
Considering that the analogous hybridized s,d energy band of Mo has the energy lower than -4 eV, the approximation of constant matrix element in Mo is at the energy -3 eV still good. The second noticeable disagreement is observed in the value $\tau_e(\mathrm{Rh})/\tau_e(\mathrm{Pd})$ at energy below 1 eV. In this case, it is related with the sudden change of the matrix element that takes place at the upper threshold of the Rh d bands with the energy near 1 eV.

Qualitatively, some of the trends in the values shown in Figs. 10, 11 can be explained by the changes in the phase space. In order to demonstrate this, we also present in Figs. 10, 11 the ratios of the phase spaces as determined by the values $S_{e,h}$. Neglecting the differences in the probabilities of the secondary electron excitations, one may suppose that $\tau(Me_1)/\tau(Me_2) \propto S(Me_2)/S(Me_1)$. As follows from the upper panel of Fig. 10, the increase of the value $\tau_e(\mathrm{Nb})/\tau_e(\mathrm{Mo})$ up to the energy about 2 eV is in correspondence with the change of the phase-space ratio $S_e(\mathrm{Mo})/S_e(\mathrm{Nb})$. So this increase of the lifetime ratio is related with the higher values of DOS in Mo just above the Fermi level, that provides more effective electron damping with the increase of the excitation energy. The value of $\tau_e(\mathrm{Rh})/\tau_e(\mathrm{Pd})$ suffers a sharp decrease in the energy interval between 0.5 and 1 eV, which can be qualitatively explained
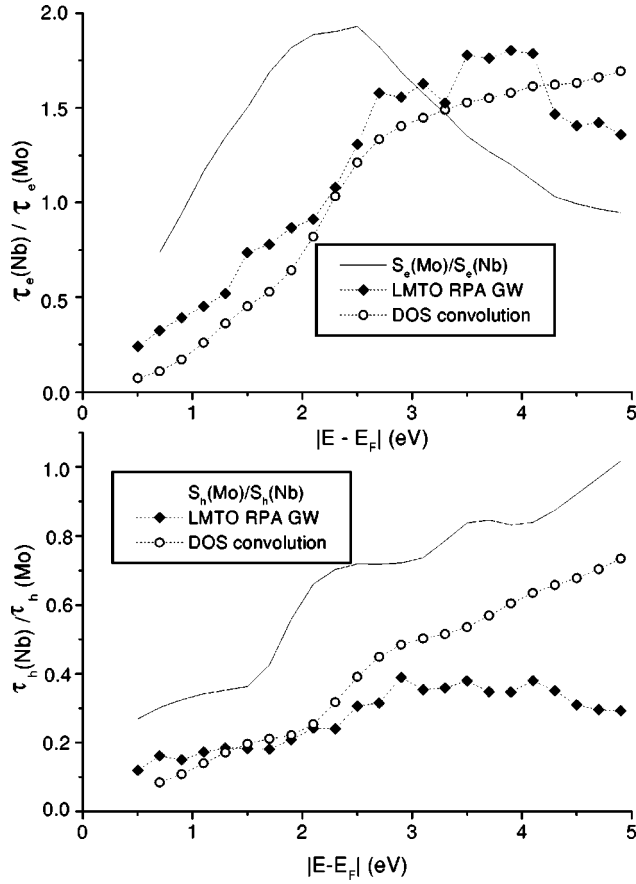
FIG. 10. The ratios of averaged electron lifetimes (upper panel) and hole lifetimes (lower panel) in Nb and Mo. The solid diamonds represent the results of the LMTO-RPA-GW calculations, whereas the open circles show the results evaluated by the DOS convolution model (see text). The solid lines illustrate the ratios of the phase-space volumes available for the electron transition (see text).

FIG. 11. The ratios of averaged electron lifetimes (upper panel) and hole lifetimes (lower panel) in Rh and Pd. Designations correspond to Fig. 10.

by the larger number of unoccupied d states in Rh providing more effective damping of the low-energy electron quasiparticles. The constant value of this ratio at higher energy is in correspondence with the invariability of the $S_e(\text{Pd})/S_e(\text{Rh})$ value. Analogous trends are observed in the changes of hole lifetimes in Rh, Pd. It is evident, however, that the ratios of lifetimes as calculated by the DOS convolution model with a constant matrix element is in noticeably better agreement with the LMTO-RPA-GW results than the evaluations based on the phase space arguments, thus demonstrating the importance of the secondary electron excitations.

The presented comparisons demonstrate that the lifetime calculations by the DOS convolution model with a fixed matrix element show in many cases a good agreement with the averaged *ab initio* lifetimes. The discussed metals display, however, significant dispersion of the lifetimes with respect to the averaged value. As an example, we show in Fig. 12 the calculated electron quasiparticles lifetimes in Nb for various **k** values, comparing them with the lifetimes in Ag. As follows from the upper panel of Fig. 12, the electron lifetimes in Ag correspond well to the FEG theory with the fitted electron-density parameter $r_s = 2.0$. At any given energy, a
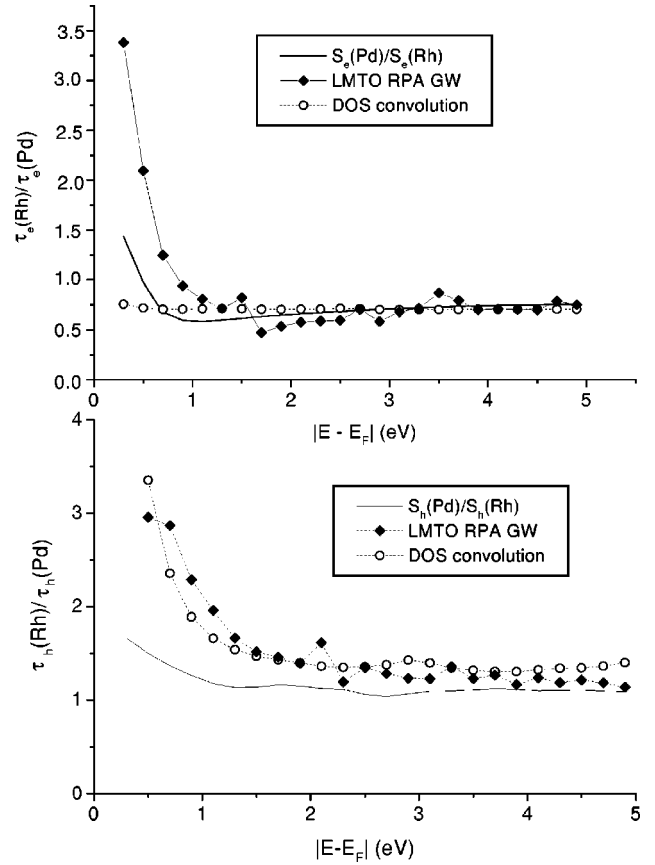
rather small dispersion of electron lifetimes with momentum is observed. More fine test on the validity of the FEG theory is provided by the energy dependence of the scaled lifetime $\tau \times (E - E_F)^2$. According to the classic works of Quinn and Ferrell,[27] Quinn,[29] Ritchie and Ashley[28] this has to be a slowly changing value, constant in the limit of small r_s. As follows from the inset in the upper panel of Fig. 12, for the energies up to 3.5 eV, the scaled lifetime generally obeys to this requirement, demonstrating rather small momentum dependence. Besides, as calculated by Eq. (1), scaled lifetime is equal to 46.5 fs eV^2, which does not deviate much from the LMTO-RPA-GW values. On the contrary, both the lifetime and scaled lifetime in Nb (as well as in Mo) reveal a very large momentum dependence thus showing an importance of the band-structure effects. The attempts to fit the lifetimes of the FEG theory to the averaged *ab initio* lifetimes by choosing the r_s value lead to rather unsatisfactory results. It is evident from Fig. 12 where we show the result of the best fitting that was obtained for Nb with $r_s = 3.1$. A similar level of the fitting accuracy is also achieved for Mo, and slightly better agreement is obtained for Rh and Pd, with $r_s = 3.5$ for Pd. The accuracy of the fitting appears to be much worse in comparison with the lifetime evaluations by the DOS convolution model, see Fig. 5.
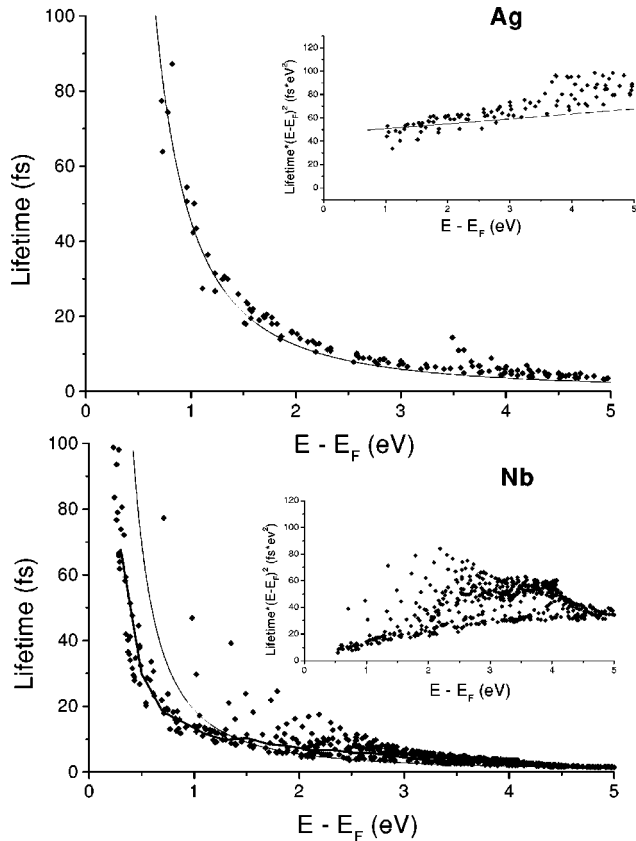
FIG. 12. The electron lifetimes (less than 100 fs) in Ag (upper panel) and Nb (lower panel) as calculated by the LMTO-RPA-GW method (solid diamonds). The insets show the energy-scaled lifetimes (diamonds). In the upper panel, the solid lines depict the averaged lifetimes and energy-scaled lifetimes. In the lower panel, the momentum-averaged LMTO-GW lifetimes are depicted by the thick solid line, whereas the thin solid line represents the lifetimes calculated by the FEG model with $r_s = 3.1$.

V. CONCLUSIONS

We report *ab initio* calculations of the dielectric functions, electron-energy loss functions and lifetimes of electron and hole excitations in Nb, Mo, Rh, Pd, that are examples of the transition metal with intermediately localized *d* states. The calculated dielectric functions and EELF are generally in good agreement with experimental data. For Mo, the calculated plasmon peak is somewhat higher in energy than the experimental one, but for Pd the agreement is very good provided that $4f$ orbitals are included in the basis.

We have analyzed the differences between the averaged lifetimes in Nb, Mo, Rh, Pd, and in noble metals, having compared with the data on Ag. At energies up to 5 eV, the electron lifetimes in Nb, Mo, Rh, Pd are much shorter due to the higher phase space available for the scattered electrons. We have also evaluated the lifetimes employing the DOS convolution model of the STA. The energy dependence and optimal value of the matrix element of the model have been estimated by comparing with the LMTO-RPA-GW calculations. In many cases the energy dependence of the matrix element is not important, and a good accordance between the DOS convolution model and LMTO-RPA-GW calculations is achieved with constant matrix element.

The phase-space arguments are found to be of limited validity in explaining the differences between the lifetimes in the metals of interest. The STA, on the other hand, is more reliable and is in good agreement with the GW lifetimes. Only in the case of Ag for energies below -3 eV the STA and GW essentially disagree due to the importance of the matrix elements.

We have calculated the ratios of the electron and hole lifetimes in the metals of interest. A generally good accordance between these ratios calculated within the LMTO-RPA-GW and within the DOS convolution model is observed. At a deeper level, the ratio $\tau_h(\mathrm{Nb})/\tau_h(\mathrm{Mo})$ calculated in STA shows a deviation from the GW above 3 eV, and similarly $\tau_e(\mathrm{Rh})/\tau_e(\mathrm{Pd})$ at energy below 1 eV. This can be traced back to the assumption of constant matrix element in STA. Compared to the results obtained from the phase-space argument, the STA results are much closer to the GW results, showing the importance of the secondary electron excitations.

Of the metals studied, the lifetime in Nb as well as in Mo reveal a large momentum dependence. Hence, although the STA is valuable for the estimations of the averaged lifetimes, the *ab initio* methods are unavoidable if a detailed knowledge about lifetimes is necessary.

[1] H. Petek and S. Ogawa, Prog. Surf. Sci. **56**, 239 (1997).

[2] J. Bokor, Science **246**, 1130 (1989); R. Hight, Surf. Sci. Rep. **21**, 275 (1995).

[3] C. A. Schmuttenmaier, M. Aeschlimann, H. E. Elsayed-Ali, R. J. D. Miller, D. A. Mantell, J. Cao, and Y. Gao, Phys. Rev. B **50**, 8957 (1994).

[4] T. Hertel, E. Knoesel, M. Wolf, and G. Ertl, Phys. Rev. Lett. **76**, 535 (1996).

[5] S. Ogawa, H. Nagano, and H. Petek, Phys. Rev. B **55**, 10 869 (1997).

[6] J. Cao, Y. Gao, R. J. D. Miller, H. E. Elsayed-Ali, and D. A. Mantell, Phys. Rev. B **56**, 1099 (1997).

[7] E. Knoesel, A. Hotzel, and M. Wolf, Phys. Rev. B **57**, 12 812 (1998).

[8] J. Cao, Y. Gao, H. E. Elsayed-Ali, R. J. D. Miller, and D. A. Mantell, Phys. Rev. B **58**, 10 948 (1998).

[9] M. Aeschlimann, M. Bauer, S. Pawlik, W. Weber, R. Burgermaister, D. Oberli, and H.-C. Siegmann, Phys. Rev. Lett. **79**, 5158 (1997).

[10] R. Knorren, K. H. Bennemann, R. Burgermeister, and M. Aeschlimann, Phys. Rev. B **61**, 9427 (2000).

[11] W. Nessler, S. Ogawa, H. Nagano, H. Petek, J. Shimoyama, Y. Nakayama, and K. Kishio, Phys. Rev. Lett. **81**, 4480 (1998).

[12] L. Hedin and S. Lundqvist, in *Solid State Physics*, edited by H.

Ehrenreich, F. Seitz, and D. Turnbull (Academic Press, New York, 1969), Vol. 23.

[13] F. Aryasetiawan and O. Gunnarsson, Rep. Prog. Phys. **61**, 237 (1998).

[14] J. C. Inkson, *Many-Body Theory of Solids* (Plenum Press, New York, 1984); A. L. Fetter and J. D. Walecka, *Quantum Theory of Many-Particle Systems* (McGraw-Hill, New York, 1971).

[15] P. M. Echenique, J. M. Pitarke, E. V. Chulkov, and A. Rubio, Chem. Phys. **251**, 1 (2000).

[16] C. N. Berglund and W. E. Spicer, Phys. Rev. **136**, 1030 (1964).

[17] E. O. Kane, Phys. Rev. **159**, 624 (1967).

[18] W. F. Krolikowsky and W. E. Spicer, Phys. Rev. **185**, 882 (1969).

[19] D. R. Penn, Phys. Rev. B **22**, 2677 (1980).

[20] D. R. Penn, S. P. Apell, and S. M. Girvin, Phys. Rev. B **32**, 7753 (1985).

[21] D. R. Penn, S. P. Apell, and S. M. Girvin, Phys. Rev. Lett. **55**, 518 (1985).

[22] D. R. Penn and S. P. Apell, Phys. Rev. B **38**, 5051 (1988).

[23] F. Passek, M. Donath, K. Ertl, and V. Dose, Phys. Rev. Lett. **75**, 2746 (1995).

[24] H.-L. Drouhin, Phys. Rev. B **56**, 14 886 (1997).

[25] H.-L. Drouhin, Phys. Rev. B **62**, 556 (2000).

[26] E. Zarate, P. Apell, and P.-M. Echenique, Phys. Rev. B **60**, 2326 (1999).

[27] J. J. Quinn, Phys. Rev. **126**, 1453 (1962).

[28] R. H. Ritchie and J. C. Ashley, J. Phys. Chem. Solids **26**, 1689 (1963).

[29] J. J. Quinn and R. A. Ferrell, Phys. Rev. **112**, 812 (1958).

[30] R. H. Ritchie, Phys. Rev. **114**, 644 (1959); J. C. Schelton, Surf. Sci. **44**, 305 (1974); L. Kleinmann, Phys. Rev. B **3**, 2982 (1971); D. R. Penn, Phys. Rev. B **13**, 5248 (1976); D. R. Penn, Phys. Rev. B **22**, 2677 (1980).

[31] C. J. Tung, J. C. Ashley, and R. H. Ritchie, Surf. Sci. **81**, 427 (1979); D. R. Penn, Phys. Rev. B **35**, 482 (1987).

[32] J. J. Quinn, Appl. Phys. Lett. **2**, 167 (1963); S. L. Adler, Phys. Rev. **130**, 1654 (1963).

[33] W.-D. Schöne, R. Keyling, M. Bandić, and W. Ekardt, Phys. Rev. B **60**, 8616 (1999).

[34] I. Campillo, J. M. Pitarke, A. Rubio, E. Zarate, and P. M. Echenique, Phys. Rev. Lett. **83**, 2230 (1999).

[35] R. Keyling, W.-D. Schöne, and W. Ekardt, Phys. Rev. B **61**, 670 (2000).

[36] I. Campillo, A. Rubio, J. M. Pitarke, A. Goldmann, and P. M. Echenique, Phys. Rev. Lett. **85**, 3241 (2000).

[37] I. Campillo, V. M. Silkin, J. M. Pitarke, E. V. Chulkov, A. Rubio, and P. M. Echenique, Phys. Rev. B **61**, 13 484 (2000).

[38] V. P. Zhukov, F. Aryasetiawan, E. V. Chulkov, I. G. de Gurtubay, and P. M. Echenique, Phys. Rev. B **64**, 195122 (2001).

[39] M. Aeschlimann, M. Bauer, and S. Pawlik, Chem. Phys. **205**, 127 (1996).

[40] W. Ekardt, W.-D. Schöne, and R. Keyling, Appl. Phys. A: Mater. Sci. Process. **71**, 529 (2000).

[41] L. I. Schiff, *Quantum Mechanics* (McGraw-Hill, London, 1985).

[42] O. K. Andersen, Phys. Rev. B **12**, 3060 (1975).

[43] O. K. Andersen, O. Jepsen, and M. Sob, Lect. Notes Phys. **283**, 1 (1987).

[44] F. Aryasetiawan and O. Gunnarsson, Phys. Rev. B **49**, 7219 (1994).

[45] F. Aryasetiawan and O. Gunnarsson, Phys. Rev. B **49**, 16 214 (1994).

[46] F. Aryasetiawan, Phys. Rev. B **46**, 13 051 (1994).

[47] T. Miyake and F. Aryasetiawan, Phys. Rev. B **61**, 7172 (2000).

[48] M. A. Cazalilla, J. S. Dolado, A. Rubio, and P. M. Echenique, Phys. Rev. B **61**, 8033 (2000).

[49] A. G. Eguiluz, J. M. Sullivan, and W. Ku, Intern. Journ. Quant. Quem. (2002, to be published).

[50] E. D. Palik, *Handbook of Optical Constants of Solids* (Academic Press, New York, 1985), Vol. 2.

[51] E. G. Maksimov, Usp. Fiz. Nauk (Physics-Uspekhi) **170**, 1033 (2000).

[52] G.-M. Fehrenbach, Phys. Rev. B **59**, 15 085 (1999).